Exercises on "strong-coupling" impurity solvers

Philipp Werner, ETH Zurich

For simplicity, we will consider a spin-less impurity coupled to a single bath site, $H = -\mu d^\dagger d + \epsilon a^\dagger a + V(d^\dagger a + a^\dagger d)$, with hybridization V, chemical potential $\mu = 0$ and impurity level energy $\epsilon = 0$ (see Fig. 1).

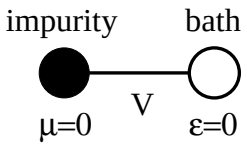

FIG. 1: Illustration of the spin-less impurity coupled to a single bath level.

In this case, the hybridization function is $\Delta(i\omega_n) = \frac{|V|^2}{i\omega_n}$, or in imaginary time

$$\Delta(\tau) = \begin{cases} -\frac{1}{2}|V|^2 & 0 < \tau < \beta \\ \frac{1}{2}|V|^2 & -\beta < \tau < 0 \end{cases} \tag{1}$$

and the impurity Green function becomes $(0 < \tau < \beta)$

$$G(\tau) = -\frac{\cosh[V(\frac{\beta}{2} - \tau)]}{2\cosh[V\frac{\beta}{2}]}. \tag{2}$$

1. Hybridization expansion

We want to understand the determinant structure in the hybridization expansion CT-QMC algorithm, and its effect on the average perturbation order and sign. Starting from the action formulation

$$Z = TrTe^{-S_{\rm loc} - \int d\tau d\tau' d^\dagger(\tau)\Delta(\tau-\tau')d(\tau')} \tag{3}$$

we obtain individual strong-coupling diagrams by expanding Z in powers of Δ.

(i) Convince yourself by looking at contributions of order $n = 1, 2, 3, \ldots$ that the weights of the $n!$ diagrams with identical operator sequence can be summed up into a determinant $|V|^{2n} \det M_n$ with

$$M_n = \begin{pmatrix} \frac{1}{2} & \frac{1}{2} & \frac{1}{2} & \cdots \\ -\frac{1}{2} & \frac{1}{2} & \frac{1}{2} & \cdots \\ -\frac{1}{2} & -\frac{1}{2} & \frac{1}{2} & \cdots \\ \cdots & \cdots & \cdots & \cdots \end{pmatrix}. \tag{4}$$

Examples for $n = 2$ are shown in Fig. 2. The thin line represents the imaginary time interval $[0, \beta]$, full dots correspond to creation operators $d^\dagger$ and open dots to annihilation operators d. Thick black segments represent the imaginary-time intervals in which an electron resides on the impurity, dashed lines the hybridization functions connecting pairs of creation and annihilation operators.

(ii) Show by induction that $\det M_n = \frac{1}{2}$, for all $n \geq 1$. The weight of a configuration with n segments is therefore $(d\tau)^{2n}|V|^{2n}\frac{1}{2}$.

(iii) To find the total contribution of configurations with perturbation order n to Z, we have to compute the corresponding "phase space", i. e. the integral ($\circ\tau_1$ means that the integral winds around the $[0, \beta]$

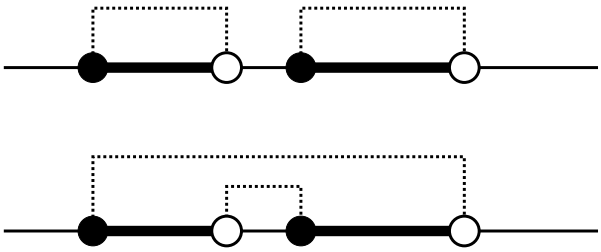

FIG. 2: Illustration of two diagrams for perturbation order $n = 2$, whose weight can be summed up into a determinant. Consider also the case where the d and $d^\dagger$ operators are exchanged.

interval)

$$I_n = \int_0^\beta d\tau_1 \int_{\tau_1}^\beta d\tau_1' \int_{\tau_1'}^\beta d\tau_2 \int_{\tau_2}^\beta d\tau_2' \ldots \int_{\tau_{n-1}'}^\beta d\tau_n \int_{\tau_n}^{\circ\tau_1} d\tau_n'. \tag{5}$$

Show that $I_n = \frac{2\beta^{2n}}{(2n)!}$, and hence that the probability distribution for the perturbation orders is

$$p(n) = \frac{1}{\cosh(\beta|V|)} \frac{(\beta|V|)^{2n}}{(2n)!}. \tag{6}$$

(iv) What would the expression for the probability distribution be if we had not resummed collections of strong-coupling diagrams into determinants, i. e. if we had sampled individual diagrams with the absolute value of their weight?

(v) Plot the results of (iii) and (iv) for several values of $\beta|V|$, and discuss what we can learn from this comparison about the efficiency of the determinant based algorithm and the sign problem in simulations based on individual diagrams.

Try to reproduce the results in Fig. 3 (for $c = \frac{|V|^2}{2}$).

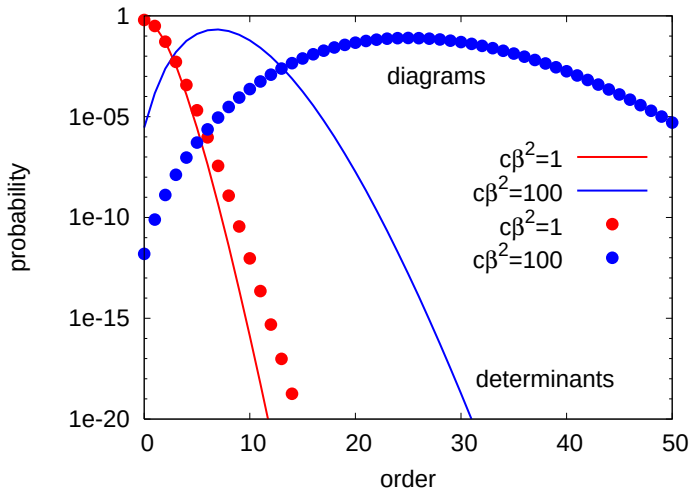

FIG. 3: Distribution of perturbation orders for algorithms sampling individual strong-coupling diagrams (dots) and determinants (lines).

1. Non-crossing approximation

In the non-crossing approximation, one only resums the strong-coupling diagrams which have *no crossing hybridization lines*. This can be done by introducing "pesudo-particle" Green functions G_0 and G_1 for the empty and occupied state, respectively, and selfconsistently solving the coupled Dyson equations

$$G_0(\tau) = g_0(\tau) + \int_0^\tau d\tau_2 \int_0^{\tau_2} d\tau_1 G_0(\tau_1)\Sigma_0[G_1](\tau_2-\tau_1)g_0(\tau-\tau_2), \tag{7}$$

$$G_1(\tau) = g_1(\tau) + \int_0^\tau d\tau_2 \int_0^{\tau_2} d\tau_1 G_1(\tau_1)\Sigma_1[G_0](\tau_2-\tau_1)g_1(\tau-\tau_2), \tag{8}$$

where $g_i(\tau) = -e^{-E_i\tau}$ is the noninteracting pseudo-particle Green function corresponding to the eigenstate of $H_{\rm loc}$ with energy E_i.

(i) Rewrite the NCA equations as integro-differential equations, and solve them iteratively using the initial condition $G_i(0) = -1$.

In the case of our simple model $E_0 = E_1 = 0$, $\Delta(\tau) = \pm\frac{1}{2}|V|^2$, so you should get

$$\partial_\tau G_0(\tau) = -\int_0^\tau d\tau_1 G_0(\tau_1)\frac{1}{2}|V|^2 G_1(\tau-\tau_1), \tag{9}$$

$$\partial_\tau G_1(\tau) = -\int_0^\tau d\tau_1 G_1(\tau_1)\frac{1}{2}|V|^2 G_0(\tau-\tau_1). \tag{10}$$

(ii) Compute the Green function from the converged pseudoparticle propagators as

$$G(\tau) = \frac{G_1(\tau)G_0(-\tau)}{G_0(\tau)+G_1(\tau)}. \tag{11}$$

(iii) Compare the NCA result to the exact Green function (2). For $\beta V = 5$, 20 you should find the Green functions plotted in Fig. 4.

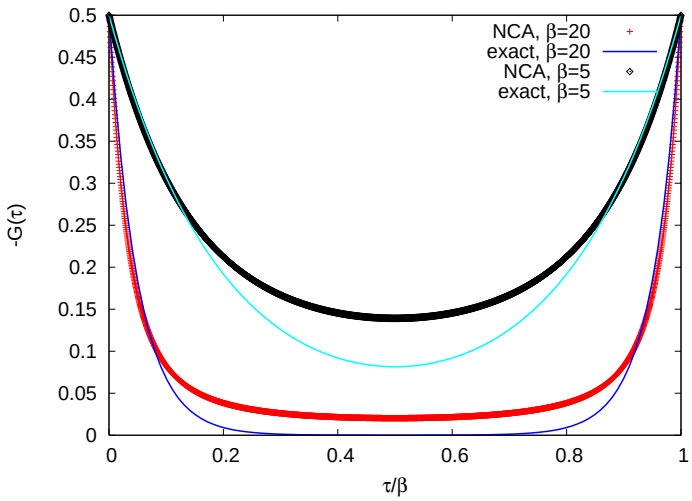

FIG. 4: Green functions for $\beta V = 5$, 20.